

A Review of Clinical and Imaging Findings in Tumefactive Demyelination

Mariko Nakayama, MD^{1,2}, Shotaro Naganawa, MD, PhD¹, Michelle Ouyang, MD³, Karra A. Jones, MD, PhD⁴, John Kim, MD¹, Aristides A. Capizzano, MD¹, Toshio Moritani, MD, PhD¹

Neuroradiology/Head and Neck Imaging · Review

Keywords

MRI, multiple sclerosis, neuromyelitis optica spectrum disorder, tumefactive demyelination

Submitted: Mar 25, 2020

Revision requested: May 29, 2020

Revision received: Jun 17, 2020

Accepted: Jun 22, 2020

First published online: May 19, 2021

The authors declare that they have no disclosures relevant to the subject matter of this article.

OBJECTIVE. Tumefactive demyelination mimics primary brain neoplasms on imaging, often necessitating brain biopsy. This article reviews the literature for the clinical and radiologic findings of tumefactive demyelination in various disease processes to facilitate identification of tumefactive demyelination on imaging.

CONCLUSION. Both clinical and radiologic findings must be integrated to distinguish tumefactive demyelinating lesions from similarly appearing lesions on imaging. Further research on the immunopathogenesis of tumefactive demyelination and associated conditions will elucidate their interrelationship.

Tumefactive demyelinating lesions are large demyelinating lesions that present with significant mass effect and surrounding edema. They are most commonly associated with multiple sclerosis (MS). However, tumefactive demyelinating lesions are also seen in other conditions, including neuromyelitis optica spectrum disorder (NMOSD), Baló concentric sclerosis (BCS), myelinoclastic diffuse sclerosis (Schilder disease), acute disseminated encephalomyelitis (ADEM), acute hemorrhagic leukoencephalitis, and autoimmune-mediated encephalitis. Tumefactive demyelinating lesions have been arbitrarily defined as demyelinating lesions greater than 2 cm on T2-weighted MRI, although smaller lesions between 0.5 and 2 cm may also show similar MRI characteristics and clinical evolution [1]. Tumefactive demyelination can manifest in isolation at the onset or during the course of other disease processes. Furthermore, its pathophysiology remains poorly understood.

Tumefactive demyelination was first reported in 1979 by van der Velden et al. [2] on unenhanced head CT of a patient with pathologically confirmed MS. Since then, tumefactive demyelinating lesions have been described by several names in the literature, including pseudotumoral demyelinating lesions, tumefactive or tumorlike MS, and tumorlike demyelinating lesions, among other designations [3]. These terms have often been used interchangeably, which may in part reflect both the diagnostic challenge of tumefactive demyelination and its elusive relationship to associated conditions, many of which have overlapping features with each other. Efforts are underway to clarify the interrelationship between tumefactive demyelination, MS, and atypical demyelinating disease processes that were previously considered subtypes of MS [4].

As its name suggests, tumefactive demyelination mimics brain tumors or other space-occupying lesions including abscess, other infections, metastasis, or infarct. The detection of tumefactive demyelination frequently leads to diagnostic uncertainty, particularly if the lesions occur in patients without a known demyelinating disease. Therefore, these cases often lead to brain biopsy to establish a diagnosis, causing an increase in morbidity, delays in treatment, and unnecessary patient distress [5] despite the fact that there are radiologic signs that can be helpful in diagnosing tumefactive demyelination. To distinguish tumefactive demyelinating lesions from neoplastic or other lesions, this article reviews the current state of the literature on clinical and radiologic findings of tumefactive demyelination and its associated diseases. The goal of this article is to facilitate identification of tumefactive demyelination on imaging.

¹Department of Radiology, University of Michigan, 1500 E Medical Center Dr, Ann Arbor, MI 48109. Address correspondence to T. Moritani (tmoritan@med.umich.edu).

²Kobe University School of Medicine, Kobe, Japan.

³Department of Radiology, University of Iowa Hospitals and Clinics, Iowa City, IA.

⁴Department of Pathology, University of Iowa Hospitals and Clinics, Iowa City, IA.

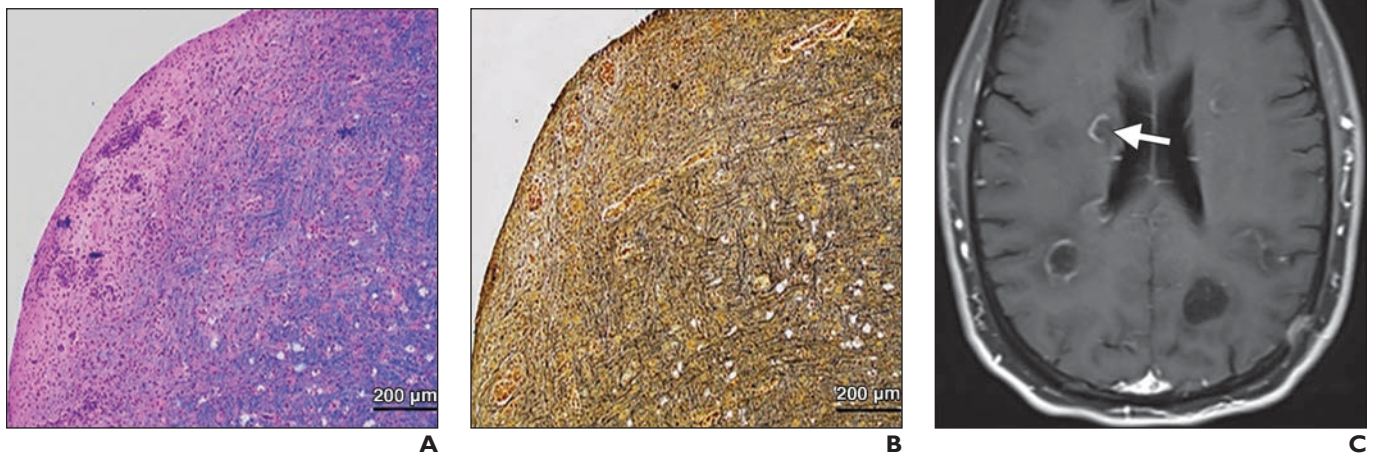


Fig. 1—63-year-old man with multiple sclerosis and tumefactive demyelination. Patient presented with acute left-sided weakness, progressively worsening gait, left foot drag, lightheadedness, and dizziness.
A, Photomicrograph (H and E) of biopsied lesion shows normal white matter on right with myelin-highlighted blue and area of demyelination on left with loss of myelin, macrophages, and perivascular lymphocytes.
B, Photomicrograph (Bielschowsky silver) shows relative axonal preservation in area corresponding to demyelination.
C, Axial contrast-enhanced T1-weighted image shows enhancing lesions with open ring pattern (*arrow*).

Epidemiology

Currently, no large-scale epidemiologic data are available on tumefactive demyelination prevalence. Several recent cohort studies reported a wide range of tumefactive demyelination prevalence among patients with MS, ranging between 1.4% (10 of 711 patients) and 8.2% (24 of 293 patients) [1, 6, 7]. These rates are higher than those reported in earlier studies (one reported 0.17% occurrence among patients with MS or chronic inflammatory disease) most likely owing to the advancement of MRI studies available [8]. Mean age of patients at tumefactive demyelination onset is between 20 and 40 years, with varying levels of female predominance [9, 10].

Clinical Manifestations

Some tumefactive demyelinating lesions are asymptomatic and are incidentally discovered on MRI scans. Symptomatic lesions present acutely or subacutely, and clinical presentations vary by the size and location of the lesion and the degree of mass effect. Hemiparesis or hemiplegia are the most common presenting symptoms (67%). However, other symptoms including aphasia, headache, visual and cognitive disturbances, and sensory disorders may also be present [10].

Pathologic Appearance

Common histopathologic findings of tumefactive demyelination resemble prototypic MS and reflect active inflammatory demyelinating disease. These include areas of demyelination with relative axonal sparing, foamy macrophages (some of which contain myelin), reactive astrocytes, and perivascular lymphocytes [11] (Figs. 1A and 1B). The presence of spared axons is important to distinguish tumefactive demyelination from a subacute infarction, which also presents with many foamy macrophages and reactive

astrocytes. This analysis can be undertaken using silver staining or neurofilament immunohistochemistry. Creutzfeldt-Peters cells are reactive astrocytes with fragmented nuclear inclusions that can be seen in tumefactive demyelination, but Creutzfeldt-Peters cells can also be found among neoplastic glial cells in glioblastomas [12].

MRI Appearance of Tumefactive Demyelination

MRI is the best imaging modality for tumefactive demyelination diagnosis (Table 1). Several characteristic conventional MRI features of tumefactive demyelination have been introduced, although diagnostic uncertainties still remain [5]. These include an open ring or incomplete rim of enhancement, a T2-hypointense rim, absent or mild mass effect, and absent or mild perilesional edema (pooled incidence of 35%, 48%, 67%, and 57%, respectively) [13]. MRI's pooled sensitivity and specificity for differentiating tumefactive demyelinating lesions from primary brain tumor have been reported as 89% and 94%, respectively [13]. Furthermore, previous reports have suggested four categories of tumefactive demyelinating lesions based on MRI appearance: ringlike, megacystic, infiltrative, and Baló-like; however, 14–17% of cases may not fit any of the categories [14, 15]. Tumefactive demyelination shows various patterns of contrast enhancement, including homogeneous, heterogeneous, patchy and diffuse, cotton-ball, closed ring, open ring, and nodular [9].

Among the aforementioned MRI features of tumefactive demyelination, the most frequently reported is an open ring of enhancement with the incomplete portion of the ring abutting the gray matter of the cortex or basal ganglia [16] (Figs. 1C and 2B). The enhancing component of the ring is regarded as an advancing front of demyelination and faces the white matter side of the lesion. The nonenhancing core in the center represents a more chronic inflammatory process [17]. On pathology, an open ring of enhancement

TABLE 1: Imaging Characteristics of Tumefactive Demyelination

Characteristic or Imaging Modality	Findings (Pooled Incidence)
Common sites of tumefactive demyelination	Frontal lobes and parietal lobes (41–74%)
CT	Hypoattenuated areas on unenhanced CT corresponding to enhancement on MRI (93%)
MRI	
T2-weighted imaging	Hypointense rim (48%) Absent or mild mass effect (67%) Absent or mild perilesional edema (57%)
Contrast-enhanced T1-weighted imaging	Open ring enhancement (35%) (Fig. 1) Closed ring enhancement (18%) Homogeneous, heterogeneous, patchy and diffuse, cotton ball, and nodular patterns of contrast enhancement
DWI	Hyperintense rim High ADC values in center of lesion and relatively low ADC values in periphery of lesion
MRS	Increased Cho/NAA ratio
¹⁸ F-FDG PET	Increased glucose uptake in lesion that is nearly equal to glucose uptake in normal cortex
Demyelinating diseases seen in association with tumefactive demyelination	
MS	Central vein sign, which is commonly seen in periventricular (94%) and deep white matter (84%) lesions (Fig. 3)
BCS	Concentric rings of T2 isointensity and hyperintensity (Fig. 4)
Myelinoclastic diffuse sclerosis	Large, masslike T2-hyperintense lesions with irregular or smooth enhancing rims in the deep and subcortical white matter (Fig. 5)
NMOSD	Often absent or minimal gadolinium enhancement

Note—MRS = MR spectroscopy, Cho = choline, NAA = *N*-acetyl aspartate, MS = multiple sclerosis, BCS = Baló concentric sclerosis, NMOSD = neuromyelitis optica spectrum disorder.

is associated with infiltration by macrophages and angiogenesis at the inflammatory border [18]. Mixed results exist about whether an open-ring or closed-ring pattern of enhancement is more common. Two cohort studies of tumefactive demyelination (with 168 and 54 cases) found that closed ring was more common. However, a recent meta-analysis showed that the pooled incidence of open-ring pattern was higher than the closed-ring pattern (35% vs 18%, respectively) [9, 13, 19]. Sensitivity of open-ring or incomplete rim enhancement for tumefactive demyelination diagnosis has been reported with significant variation (27–71%), although specificity has been consistently high (98–100%) [20–22].

Most tumefactive demyelinating lesions are supratentorial, with frontal lobe (incidence between 40.7 and 56%) and parietal lobe (reported incidence between 42 and 74.1%) being the most common sites [9, 19, 23, 24]. Corpus callosum, occipital, and temporal lobe involvement are also seen [9, 19, 23, 24]. When the corpus callosum is involved, a butterfly appearance can be seen in 12% of cases [9]. The addition of unenhanced CT to contrast-enhanced MRI may be useful to better distinguish tumefactive demyelinating lesions from tumors. Hypoattenuated areas on CT that correspond to areas of enhancement on MRI occur at a much higher rate in tumefactive demyelination than in tumor (93% vs 4%); thus, CT plus MRI showed stronger diagnostic accuracy than MRI alone (97% vs 73.0%), with a sensitivity of 87% and specificity of 100% [21].

Diffusion-Weighted MRI

The use of ADC values has been investigated to distinguish tumefactive demyelinating lesions from primary brain neoplasms.

Tumefactive demyelinating lesions show heterogeneous ADC values: high ADC in the center of the lesion due to vasogenic edema and myelin destruction and low ADC peripherally due to inflammatory cell infiltrates [25]. On serial MRI scans, restricted diffusion at the advancing edge of demyelination can evolve dynamically, which is not seen in abscesses or tumors [26]. Within the enhancing part of the lesion, tumefactive demyelination may show reduced isotropic component of the diffusion-tensor (*p*) compared with high-grade gliomas. Furthermore, the mean value of anisotropic component of diffusion-tensor (*q*) is reduced in tumefactive demyelination compared with gliomas, which may suggest greater myelin loss [22]. Although enhancing regions of tumefactive demyelination show lower ADC value than gliomas, minimum ADC values may be higher in tumefactive demyelinating lesions than in lymphomas [20, 27]. A study suggests that the minimum ADC value may be the best indicator for distinguishing tumefactive demyelinating lesions from primary CNS lymphomas, with a threshold of $0.556 \times 10^{-3} \text{ mm}^2/\text{s}$ having a sensitivity of 81.3% and specificity of 88.9% [28]. Finally, compared with high-grade gliomas, the peripheral enhancing portion of tumefactive demyelination shows higher fractional anisotropy but lower mean diffusivity values [29].

Dynamic Susceptibility Contrast Perfusion MRI

The few studies that have compared regional cerebral blood volume (rCBV) of tumefactive demyelinating lesions with the rCBV of intracranial neoplasms have shown mixed results. Tumefactive demyelinating lesions may show lower or similarly

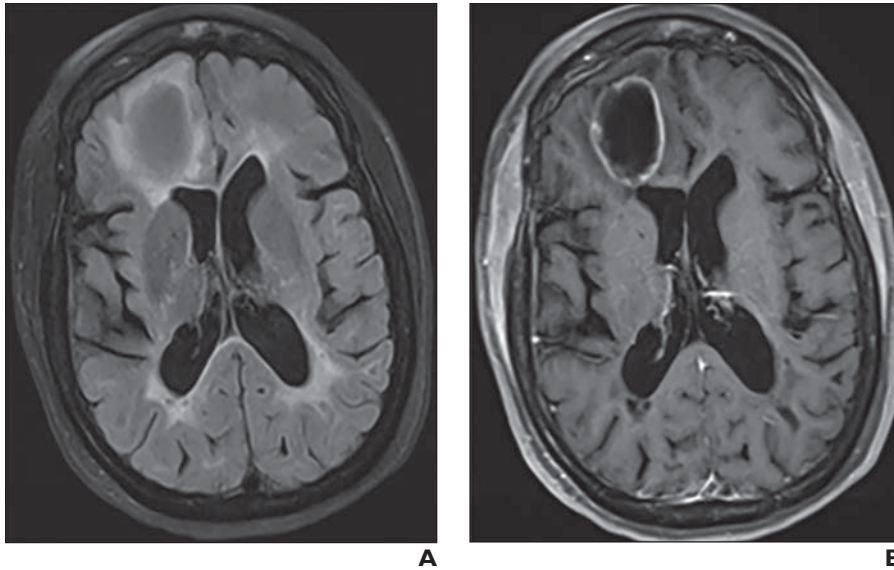


Fig. 2—50-year-old woman with multiple sclerosis and tumefactive demyelinating lesion. Patient presented with seizure without return to baseline mentation.

A, Axial FLAIR image shows large right frontal lesion with hyperintense rim and isointense center.

B, Axial contrast-enhanced T1-weighted image shows lesion has incomplete ring of enhancement.

increased rCBV compared with intracranial neoplasms [30, 31]. However, given the small sample sizes of these studies [30, 31], this issue warrants further research.

MR Spectroscopy

On MR spectroscopy (MRS), tumefactive demyelinating lesions may show an increased choline (Cho)-containing peak and a decreased *N*-acetyl aspartate (NAA) peak (i.e., an increased Cho/NAA ratio). Although this pattern can also be seen in neoplasms, two small cohort studies found an almost-identical cutoff of Cho/NAA ratio of greater than 1.72 or 1.73 as an indicator of high-grade gliomas rather than tumefactive demyelinating lesions [32, 33]. However, the applicability of this cutoff is questionable given that MRS is affected by technical factors, such as choice of sequence and TE, as well as the age of the lesion [32] and voxel positioning. Furthermore, at in vivo MRS resolution, the Cho resonance includes phosphoesters of Cho that are increased with both membrane synthesis and turnover [34]. A study with a larger sample is needed to determine the utility of MRS; however, when used as an adjunct to conventional MRI, Cho/NAA ratio has been shown to improve diagnosis [33]. Some studies have shown that a lactate peak and glutamate-glutamine peak may also be present in tumefactive demyelinating lesions [25, 35].

PET Scans

Few studies have explored the utility of ^{18}F -FDG (FDG) PET in tumefactive demyelination diagnosis. Although one study found a decrease in total brain glucose metabolism among patients with MS [36], another showed increased glucose uptake in stable MS lesions [37]. Compared with the normal cortex, tumefactive demyelinating lesions may show almost equal glucose uptake to increased glucose uptake on FDG PET [37]. Furthermore, glucose uptake of tumefactive demyelinating lesions may not significantly differ from malignant gliomas [38].

With regard to ^{11}C -methionine PET, methionine uptake of tumefactive demyelinating lesions may vary from high uptake in the entire lesion, thus mimicking a malignant tumor, to insignificant uptake [39–42]. Finally, according to a recent study, ^{18}F -fluoroeth-

yl-*l*-tyrosine PET may differentiate tumefactive demyelinating lesions from true neoplastic lesions using lesion-to-background ratio and lower SUV_{max} [43].

CSF Biochemistry

Tumefactive demyelinating lesions that occur in isolation showed IgG oligoclonal bands positivity between 52.1% and 70% of cases, and some of these patients later eventually developed MS [10, 19]. On the other hand, 90% of MS patients with tumefactive demyelinating lesions show IgG oligoclonal band positivity [19].

Conditions Associated With Tumefactive Demyelination

This section describes conditions that have been reported in association with tumefactive demyelination. Many have overlapping features that complicate diagnosis and their categorization as distinct or related conditions. Although their exact nosology remains unclear, recognition of these syndromes to be associated with tumefactive demyelination is crucial for proper tumefactive demyelination diagnosis and treatment.

Tumefactive Demyelination Associated With Multiple Sclerosis

Recent literature often describes tumefactive demyelination associated with MS as MS with an atypical presentation. Pathologic analysis of these lesions reveals active demyelination in accordance with a typical MS lesion [44]. Among patients with an established MS diagnosis, between 0.1% and 8.2% develop tumefactive demyelination [1, 6, 7, 9, 14, 19, 45]. On the other hand, between 22% and 70% of inaugural isolated tumefactive demyelination (tumefactive demyelination without any other MS lesion on the first MRI) is followed by MS, with a 5-year risk of MS conversion estimated at 27% [44]. Tumefactive demyelination-onset MS presents with an acute onset and a relapsing-remitting evolution, similar to typical MS, and does not have a worse prognosis than classic MS [10].

On imaging, tumefactive demyelination in MS has been reported in association with a central vessel sign and decreased

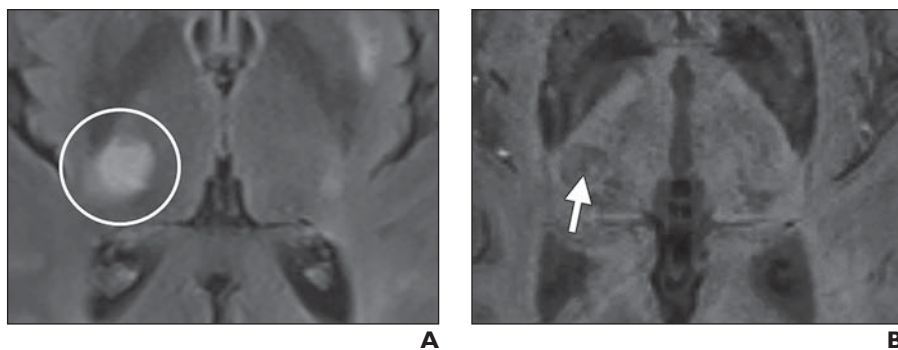


Fig. 3—63-year-old man (same patient as in Fig. 1) with multiple sclerosis and tumefactive demyelinating lesion. Patient presented with left-sided weakness, left foot drag, and gait abnormality over few months. Patient also complained of lightheadedness and dizziness.

A, Magnified axial FLAIR image shows hyperintense lesion (*circle*) in right posterior internal capsule and posterolateral thalamus.

B, Magnified axial susceptibility-weighted image shows hypointense linear vessel running through center of lesion (*arrow*).

perfusion in comparison with tumors and normal-appearing white matter. It has been hypothesized that the central vessel represents a vein draining toward distended subependymal veins [31, 46].

The presence of a central vein within the white matter lesion, called the “central vein sign” (CVS), is a specific biomarker of perivenous inflammatory demyelination. CVS is defined as a hypointense thin line or small dot (< 2 mm) that is visible in at least two planes and located centrally within the surrounding lesion on susceptibility-weighted images or T2*-weighted images (Fig. 3). Studies have found CVS in up to 80–92% of all MS lesions, and the CVS has been proposed as a potential diagnostic tool for MS [47–49]. One study reported that when more than 54% of the lesions on any given scan showed the CVS, MS diagnosis accuracy was 94% with a sensitivity of 90% and specificity of 100% [48].

Given the association of CVS with MS, MS should be a leading consideration when a CVS is found within a large tumefactive lesion suspicious for tumefactive demyelination. CVS is most commonly seen in periventricular (94%) and deep white matter (84%) lesions and decreases closer to the cortex [50–52]. A recent study described CVS associated with inflammation-dependent vascular remodeling of small to medium-sized veins, consisting of luminal enlargement and eccentric thickening of perivascular space with fibrillar collagen type I deposition [53].

Tumefactive Demyelination Associated With Baló Concentric Sclerosis

BCS is a form of atypical demyelination characterized radiologically and pathologically by concentric rings of demyelination and remyelination [54] (Fig. 4). BCS is now widely considered to occur in the context of other demyelinating processes rather than as a distinct demyelinating disease [5]. On MRI, alternating concentric rings of T2 isointensity and hyperintensity are seen, representing areas of relatively preserved myelin and demyelination, respectively [55, 56]. BCS is seen in many diseases including MS, NMOSD, progressive multifocal leukoencephalopathy, cerebral autosomal dominant arteriopathy with subcortical infarcts and leukoencephalopathy (CADASIL), and concomitant active hepatitis C and human herpesvirus 6 [57–60]. However, aside from the concentric appearance, BCS-associated tumefactive demyelination and MS-associated tumefactive demyelination show significant overlap. The advent of MRI has revealed a close link of tumefactive demyelination, BCS, and typical MS [4]. Multiple BCS lesions can coalesce to form tumefactive demyelination, and conversely, tumefactive demyelination can evolve into BCS [61, 62]. Meanwhile, a recent CSF study found significant difference in CSF findings between BCS and typical MS, suggesting that a BCS lesion may denote the presence of an immunologically distinct disease entity other than MS [63].

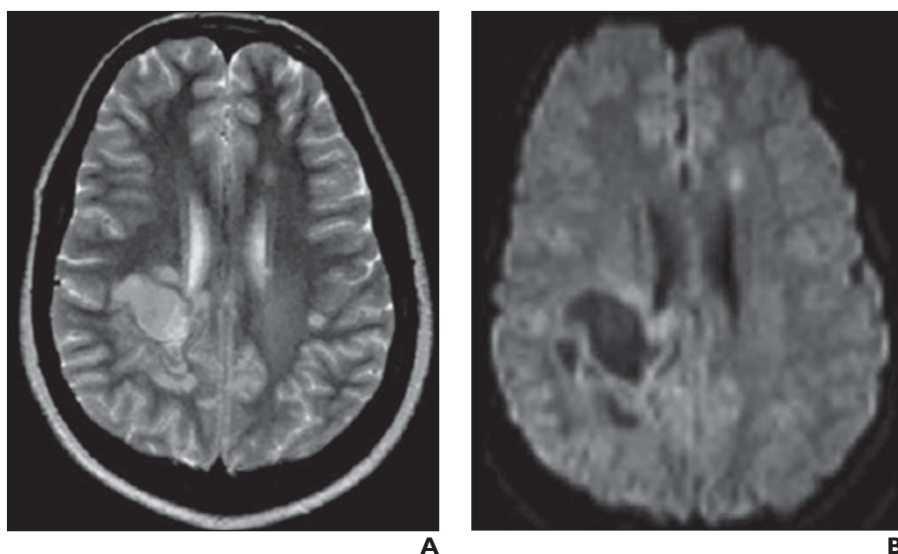


Fig. 4—17-year-old girl with biopsy-proven Baló concentric sclerosis (BCS). Patient presented with strokelike symptoms [54]. (Reprinted by permission from Springer Nature Customer Service Centre GmbH: Springer Nature *Diffusion-weighted MR imaging of the brain*, 2nd ed. by Moritani T, Ekholm S, Westesson PA [Moritani T, Ekholm S, Westesson PA, eds.] © 2009)

A, Axial T2-weighted image shows large hyperintense mass with multilayered appearance in right posterior periventricular and deep white matter.

B, Axial DW image obtained at follow-up 2 months after **A** shows lesions as hypointense with increased ADC (not shown).

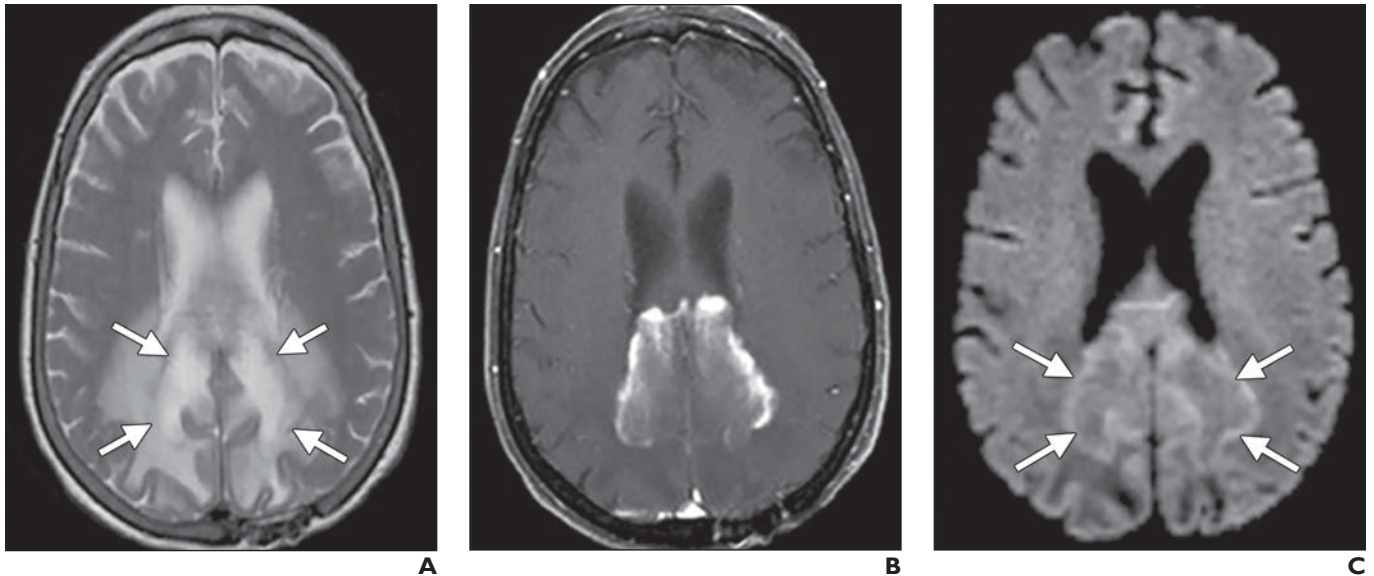


Fig. 5—80-year-old woman with biopsy-proven myelinoclastic diffuse sclerosis (Schilder disease). Patient initially presented with confusion [54]. (Reprinted by permission from Springer Nature Customer Service Centre GmbH: Springer Nature *Diffusion-weighted MR imaging of the brain*, 2nd ed. by Moritani T, Ekholm S, Westesson PA [Moritani T, Ekholm S, Westesson PA, eds.] © 2009)

A, Axial T2-weighted image shows symmetric large hyperintense lesions with slightly low-signal curvilinear areas (arrows) involving posterior corpus callosum and occipital white matter bilaterally.

B, Axial contrast-enhanced T1-weighted image shows symmetric irregular enhancement along curvilinear T2-hypointense signal areas.

C, Axial DW image shows curvilinear areas (arrows) as mildly hyperintense with decreased ADC (not shown), corresponding to active demyelination.

Tumefactive Demyelination Associated With Myelinoclastic Diffuse Sclerosis (Schilder Disease)

Myelinoclastic diffuse sclerosis, also known as Schilder disease, is a rare primary demyelinating disorder that is regarded as an MS variant that often develops during childhood and adolescence but that can occur in adults. Schilder plaques have been defined to be at least 3×2 cm in two of three dimensions and typically involve the centrum semiovale and the corpus callosum [64, 65]. MRI shows large, masslike T2-hyperintense lesions with irregular or smooth enhancing rims in the deep and subcortical white matter [54] (Fig. 5). The open-ring sign is common and is helpful in diagnosing tumefactive demyelinating lesions when present. Because Schilder disease lesions often do not seem to differ from multifocal tumefactive demyelinating lesions, some no longer consider Schilder disease to be a distinct form of atypical demyelination [5]. Pathology of Schilder disease may be identical to that of MS [64]. However, a recent CSF study showed that oligoclonal band patterns of Schilder disease are substantially different from MS, prompting authors to suggest that the two are immunologically distinct entities [66].

Tumefactive Demyelination Associated With NMOSD

NMOSD is a new disease spectrum now regarded as a distinct entity from MS. Its most significant clinical features include optic neuritis and longitudinal myelitis affecting three or more vertebral segments, and patients may or may not be seropositive for aquaporin 4 antibody (AQP4-Ab). AQP4-Ab is a pathogenic autoantibody targeting the water channel protein aquaporin 4 on astrocytic foot processes [67]. The common clinical picture of NMOSD has a significant overlap with MS and includes subacute vision loss, paraparesis or quadriparesis episodes, and relapsing attacks of varying frequency. Among patients with AQP4-Ab-se-

ronegative NMOSD, up to 25% may be seropositive for antibodies against myelin-oligodendrocyte glycoprotein (MOG-IgG), a myelin-targeting antibody [68]. MOG-IgG-seropositive NMOSD cases are now considered to denote a distinct disease entity separate from AQP4-Ab-positive NMOSD, often referred to as MOG-IgG-associated encephalomyelitis [69]. Tumefactive demyelination has been reported in association with NMOSD and MOG-IgG demyelinating diseases [45, 70, 71]. Furthermore, tumefactive demyelination has been reported to develop among patients with NMOSD who were initially misdiagnosed as having MS and were treated with interferon- β therapy and fingolimod [72].

On imaging, tumefactive demyelination-associated NMOSD often shows absent or minimum gadolinium enhancement, suggesting preserved integrity of the blood-brain barrier [73, 74], while the presence of tumefactive demyelination in NMOSD with incomplete ring enhancement may be easily confused with tumefactive demyelination in MS [75] (Fig. 6). A common MRI finding includes hyperintense lesions on T2-weighted imaging, iso- to hypointense lesions on T1-weighted imaging, and hypo- or isointense lesions on DWI with increased ADC values. If DWI hyperintensity is present, it is often due to T2 shine-through. An MRS study with a small cohort found that tumefactive demyelinating lesions in patients with NMOSD showed increased Cho/creatine ratios and decreased NAA/creatine ratios [76].

Imaging findings of AQP4-Ab-seropositive NMOSD include severe optic neuritis that may involve the optic chiasm as well as longitudinally extensive myelitis involving more than three vertebral segments, commonly in the central gray matter. Involvement of the area postrema in the dorsal medulla with intractable hiccup, nausea, and vomiting are highly specific findings [77]. Gadolinium-enhancing lesions may have a cloudlike appearance (i.e., patchy enhancing lesions that have blurred margins) in up to 90% of patients [78].

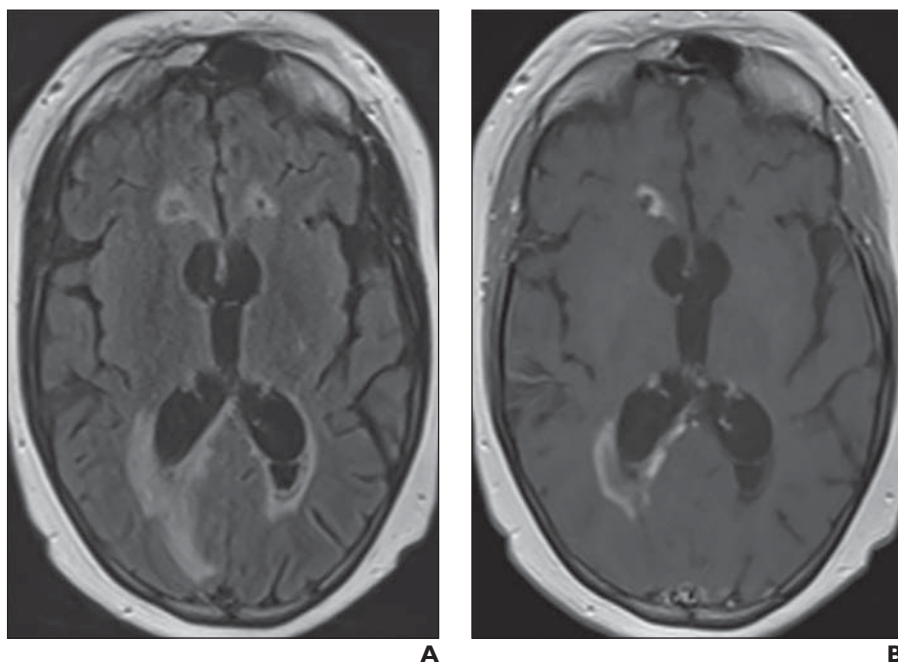


Fig. 6—35-year-old woman with anti-aquaporin 4 antibody–seropositive neuromyelitis optica spectrum disorder and tumefactive demyelinating lesion. Patient is paraplegic and presented with increased sleepiness and decreased alertness.

A, Axial FLAIR image shows multiple hyperintense lesions in periventricular regions, worse along occipital horn of right lateral ventricle. There is also hydrocephalus that required ventriculostomy placement.

B, Axial contrast-enhanced T1-weighted image shows incomplete peripheral enhancement of right-sided lesions.

Tumefactive Demyelination Associated With Acute Disseminated Encephalomyelitis

ADEM is an immune-mediated inflammatory demyelinating disorder that is typically precipitated by viral infections or vaccinations [79]. It is mostly seen in the pediatric population, with reported incidence varying between 0.4/100,000/year under the age of 20 years and 0.64/100,000/year under the age of 15 years [80, 81]. Reports of tumefactive demyelination in association with ADEM are limited, but a study with a large cohort found that 10.3% of patients had tumefactive demyelination [81]. Inflammatory demyelinating lesions of ADEM partially or completely resolve, and the occurrence of new lesions is rare at 5–8% [79].

The neurologic findings of ADEM reflect multifocal involvement, but ADEM usually behaves as a monophasic disease [80]. Classic MRI findings of ADEM on FLAIR images are multiple asym-

metric areas of hyperintensity involving white matter [54] (Fig. 7). However, size, location, and presence or absence of hemorrhage can be variable. Demyelinating lesions of ADEM almost always occur in the subcortical white matter, but they are also seen in the brainstem, spinal cord, thalami, and basal ganglia; 3.3% of ADEM cases have reportedly converted to MS [82].

Tumefactive Demyelination Associated With Other Disorders

Autoimmune-mediated encephalitis, which can be paraneoplastic, may also present with tumefactive demyelination–type lesions on imaging. We encountered a case of pathologically confirmed tumefactive demyelination associated with anti-Ma2–seropositive autoimmune encephalitis in a patient with mediastinal nonseminomatous germ cell tumor (Fig. 8). Anti-N-methyl-D-aspartate encephalitis is a subtype of autoimmune-mediated

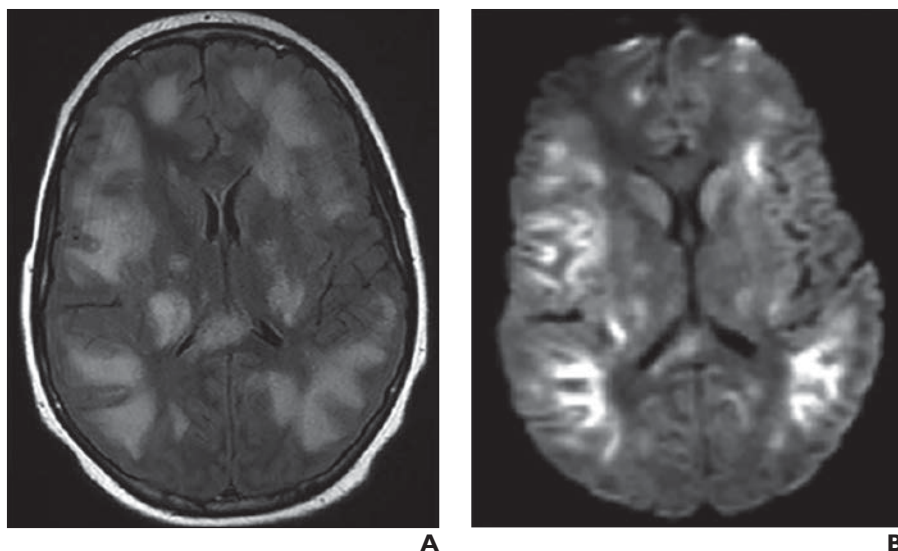


Fig. 7—11-year-old boy with acute demyelinating encephalomyelitis and tumefactive demyelinating lesion. Patient presented with altered mental status [54]. (Reprinted by permission from Springer Nature Customer Service Centre GmbH: Springer Nature *Diffusion-weighted MR imaging of the brain*, 2nd ed. by Moritani T, Ekholm S, Westesson PA [Moritani T, Ekholm S, Westesson PA, eds.] © 2009)

A, Axial FLAIR image shows multiple ill-defined hyperintense lesions in white matter, corpus callosum, basal ganglia, and thalami.

B, DW image shows multiple hyperintense lesions with increased ADC and partially decreased ADC in peripheral area of lesions, likely representing combination of vasogenic cytotoxic edema with demyelination.

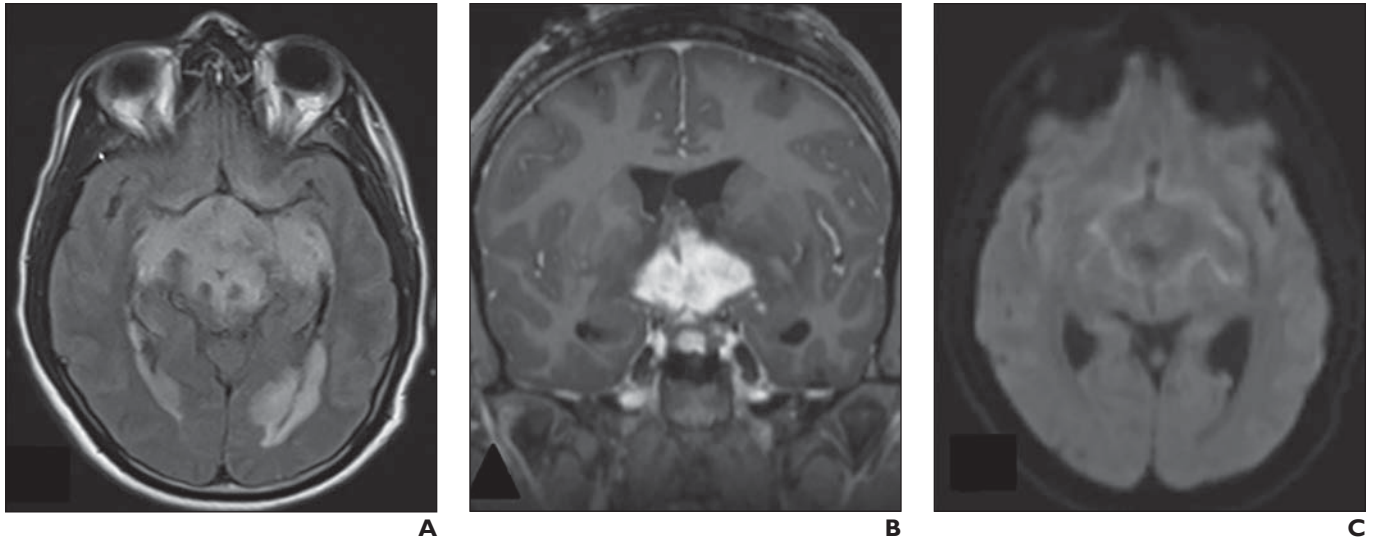


Fig. 8—30-year-old man with tumefactive demyelinating lesion associated with anti-Ma2-seropositive autoimmune encephalitis and nonseminomatous germ cell tumor. Patient presented with altered mental status, incontinence, and headache.
A, Axial FLAIR image shows extensive edema extending from hypothalamus to temporal lobes and insula bilaterally.
B, Coronal contrast-enhanced T1-weighted image shows avid enhancement in hypothalamus and basal ganglia.
C, Axial DW image shows restricted diffusion along periphery.

encephalitis associated with MRI and pathologic changes of demyelination [83]. This type of encephalitis has been associated with NMOSD, and its MRI appearance may mimic tumefactive demyelination [84, 85]. Furthermore, tumefactive demyelination has been reported as a potential adverse event of fingolimod or natalizumab use in MS and NMOSD [86–88].

It is also important to be aware that tumefactive demyelination can be a harbinger of malignancy. Pathologically confirmed tumefactive demyelinating lesions, after showing good response to corticosteroids, can precede primary CNS lymphoma in immunocompetent patients [89–92]. A biopsied lesion showing demyelination may later prove to be a rapidly developing primary CNS lymphoma. CNS lymphoma has been described in patients treated with mycophenolic acid for systemic lupus erythematosus, which may originally present as demyelinating lesions [93]. Awareness of this possible disease course is important to miti-

gate disease progression, and diligent follow-up is required in tumefactive demyelination regardless of steroid responsiveness.

Tumefactive Demyelination Associated With Developmental Venous Anomalies

Developmental venous anomalies (DVAs) are the most common type of congenital cerebral vascular malformations and are generally regarded as benign and incidental developmental anomalies. However, between 11.6% and 28.3% of DVAs are associated with FLAIR hyperintensity in the DVA drainage territory of the brain parenchyma [94–97]. Although the exact pathophysiology of DVA-associated signal-intensity change remains unclear, it has been hypothesized that DVA causes impaired venous drainage, which predisposes to blood-brain barrier breakdown and increases lymphocytic infiltration in adjacent brain parenchyma, leading to demyelination. A recent study found that

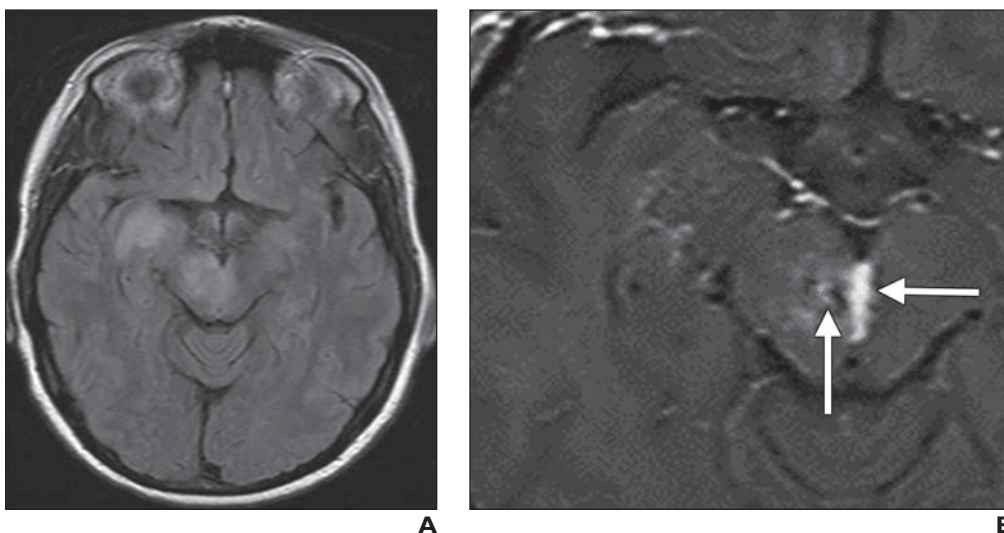


Fig. 9—56-year-old woman with biopsy-proven tumefactive demyelinating lesion associated with developmental venous anomaly (DVA). Patient presented with diplopia, acute left eyelid droop, and right-hand tingling and numbness.
A, Axial FLAIR image shows hyperintense lesion in right insula and right midbrain.
B, Magnified axial contrast-enhanced T1-weighted image shows patchy peripheral enhancement of lesion. Note “central vein” sign (vertical arrow) and associated DVA (horizontal arrow).

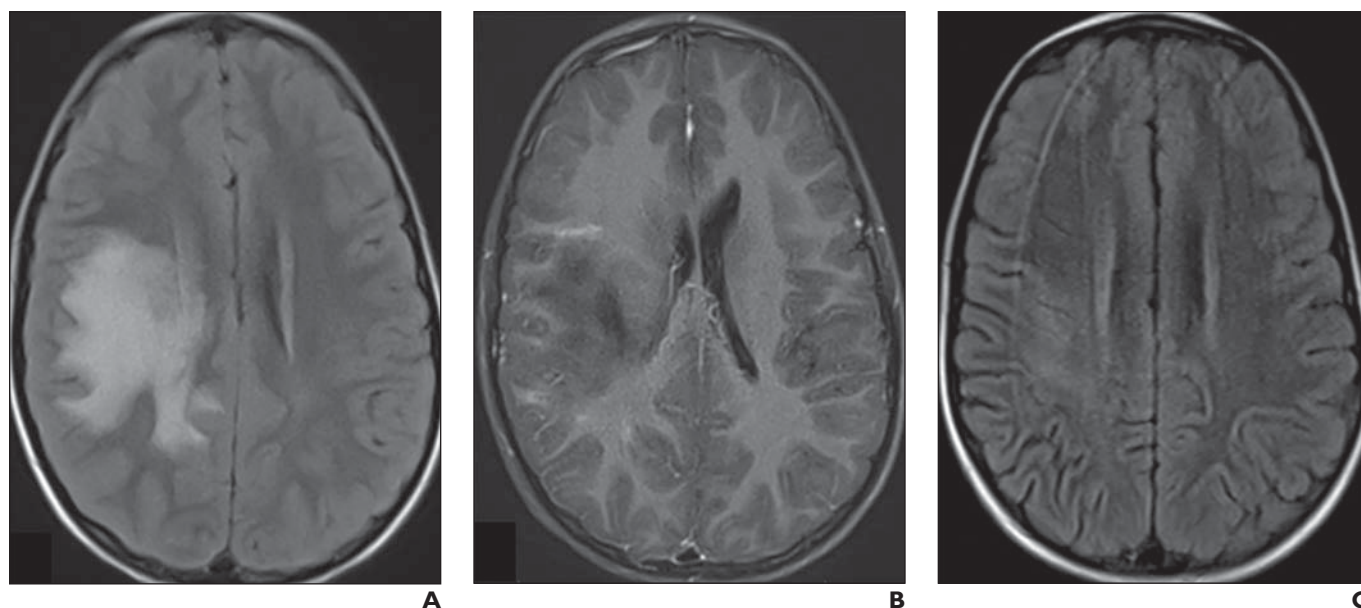


Fig. 10—8-year-old boy with large tumefactive demyelinating lesion. Patient presented with left-sided weakness and headache. Patient showed good response to corticosteroid treatment.

A, Axial FLAIR image shows large hyperintense lesion in right frontal and parietal lobes.

B, Axial contrast-enhanced T1-weighted image shows incomplete peripheral enhancement of lesion.

C, Axial FLAIR image obtained after patient had received 5 weeks of corticosteroid treatment shows decreased signal abnormality in right frontal and parietal lobes.

47.3% of DVAs in patients with MS were associated with FLAIR hyperintense signal that showed a positive CVS (Fig. 9). This finding prompted the authors to suggest that a demyelinating cause should be considered when a tumefactive demyelinating lesion with CVS is found in close association with a DVA [98]. Because the DVA may be the sole venous outflow to adjacent normal brain parenchyma, biopsy of a suspected tumefactive demyelinating lesion in close proximity to DVA should be avoided due to increased hemorrhage and infarction risks [99].

Management and Course of Tumefactive Demyelination

Management recommendations for isolated tumefactive demyelinating lesions are based on case reports and series. Simple observation is sufficient for asymptomatic or minimally symptomatic cases, and follow-up MRI at 4–6 weeks (or sooner if symptoms worsen) is considered reasonable. High-dose IV corticosteroids are the first-line treatment of acute symptomatic tumefactive demyelinating lesions [19] (Fig. 10). When corticosteroids are ineffective, plasma exchange therapy can be considered [100]. When lesions progress further despite treatment, good response has been shown with cyclophosphamide and rituximab [5]. When MS evolves or when tumefactive demyelinating lesions present with typical MS, it is reasonable to treat with MS disease-modifying therapy [101]. Caution is required for the use of fingolimod, but no evidence exists regarding the preferred type of MS therapy. Relapses of tumefactive demyelinating lesions are said to occur in approximately 17% of isolated tumefactive demyelinating lesions, which are also treated with corticosteroids [19]. The long-term prognosis of tumefactive demyelinating lesions warrants further research and may largely depend on the underlying immunopathology.

Conclusion

Tumefactive demyelination is an uncommon but important manifestation of multiple immune-mediated neurologic diseases that can be difficult to diagnose. However, identifying an abnormality as demyelination rather than malignancy or infection is critical in guiding further workup and treatment. To do so, integrating clinical findings with findings from multiple imaging modalities is essential. Continued research to understand the immunopathogenesis of tumefactive demyelination as well as its associated diseases will aid in further understanding their interrelationship and nosology.

References

1. Patriarca L, Torlone S, Ferrari F, et al. Is size an essential criterion to define tumefactive plaque? MR features and clinical correlation in multiple sclerosis. *Neuroradiol J* 2016; 29:384–389
2. van der Velden M, Bots GT, Endtz LJ. Cranial CT in multiple sclerosis showing a mass effect. *Surg Neurol* 1979; 12:307–310
3. Algahtani H, Shirah B, Alassiri A. Tumefactive demyelinating lesions: a comprehensive review. *Mult Scler Relat Disord* 2017; 14:72–79
4. Hardy TA, Tobin WO, Lucchinetti CF. Exploring the overlap between multiple sclerosis, tumefactive demyelination and Baló's concentric sclerosis. *Mult Scler* 2016; 22:986–992
5. Hardy TA. Pseudotumoral demyelinating lesions: diagnostic approach and long-term outcome. *Curr Opin Neurol* 2019; 32:467–474
6. Sánchez P, Meca-Lallana V, Barbosa A, Manzanares R, Palmí I, Vivancos J. Tumefactive demyelinating lesions of 15 patients: clinico-radiological features, management and review of the literature. *J Neurol Sci* 2017; 381:32–38
7. Totaro R, Di Carmine C, Splendiani A, et al. Occurrence and long-term outcome of tumefactive demyelinating lesions in multiple sclerosis. *Neurol Sci* 2016; 37:1113–1117

8. Poser S, Lürer W, Bruhn H, Frahm J, Brück Y, Felgenhauer K. Acute demyelinating disease: classification and non-invasive diagnosis. *Acta Neurol Scand* 1992; 86:579–585
9. Lucchinetti CF, Gavriloa RH, Metz I, et al. Clinical and radiographic spectrum of pathologically confirmed tumefactive multiple sclerosis. *Brain* 2008; 131:1759–1775
10. Balloy G, Pelletier J, Suchet L, et al.; Société Francophone de la Sclérose en Plaques. Inaugural tumor-like multiple sclerosis: clinical presentation and medium-term outcome in 87 patients. *J Neurol* 2018; 265:2251–2259
11. Hu W, Lucchinetti CF. The pathological spectrum of CNS inflammatory demyelinating diseases. *Semin Immunopathol* 2009; 31:439–453
12. Ballester LY, Boghani Z, Baskin DS, et al. Creutzfeldt astrocytes may be seen in IDH-wildtype glioblastoma and retain expression of DNA repair and chromatin binding proteins. *Brain Pathol* 2018; 28:1012–1019
13. Suh CH, Kim HS, Jung SC, Choi CG, Kim SJ. MRI findings in tumefactive demyelinating lesions: a systematic review and meta-analysis. *AJNR* 2018; 39:1643–1649
14. Wallner-Blazek M, Rovira A, Fillipp M, et al. Atypical idiopathic inflammatory demyelinating lesions: prognostic implications and relation to multiple sclerosis. *J Neurol* 2013; 260:2016–2022
15. Seewann A, Enzinger C, Filippi M, et al.; MAGNIMS Network. MRI characteristics of atypical idiopathic inflammatory demyelinating lesions of the brain: a review of reported findings. *J Neurol* 2008; 255:1–10
16. Masdeu JC, Quinto C, Olivera C, Tenner M, Leslie D, Visintainer P. Opening imaging sign: highly specific for atypical brain demyelination. *Neurology* 2000; 54:1427–1433
17. Given CA 2nd, Stevens BS, Lee C. The MRI appearance of tumefactive demyelinating lesions. *AJR* 2004; 182:195–199
18. Kobayashi M, Shimizu Y, Shibata N, Uchiyama S. Gadolinium enhancement patterns of tumefactive demyelinating lesions: correlations with brain biopsy findings and pathophysiology. *J Neurol* 2014; 261:1902–1910
19. Altintas A, Petek B, Isik N, et al. Clinical and radiological characteristics of tumefactive demyelinating lesions: follow-up study. *Mult Scler* 2012; 18:1448–1453
20. Mabray MC, Cohen BA, Villanueva-Meyer JE, et al. Performance of apparent diffusion coefficient values and conventional MRI features in differentiating tumefactive demyelinating lesions from primary brain neoplasms. *AJR* 2015; 205:1075–1085
21. Kim DS, Na DG, Kim KH, et al. Distinguishing tumefactive demyelinating lesions from glioma or central nervous system lymphoma: added value of unenhanced CT compared with conventional contrast-enhanced MR imaging. *Radiology* 2009; 251:467–475
22. Hiremath SB, Muraliedharan A, Kumar S, et al. Combining diffusion tensor metrics and DSC perfusion imaging: can it improve the diagnostic accuracy in differentiating tumefactive demyelination from high-grade glioma? *AJNR* 2017; 38:685–690
23. Fontes-Villalba AA, French HH, Parratt JDE. Characterisation of tumefactive demyelinating lesions. *J Neurol Neurosurg Psychiatry* 2017; 88:e1.9
24. Razek AAKA, Elsebaie NA. Imaging of fulminant demyelinating disorders of the central nervous system. *J Comput Assist Tomogr* 2020; 44:248–254
25. Malhotra HS, Jain KK, Agarwal A, et al. Characterization of tumefactive demyelinating lesions using MR imaging and in-vivo proton MR spectroscopy. *Mult Scler* 2009; 15:193–203
26. Abou Zeid N, Pirko I, Erickson B, et al. Diffusion-weighted imaging characteristics of biopsy-proven demyelinating brain lesions. *Neurology* 2012; 78:1655–1662
27. Wen JB, Huang WY, Xu WXZ, Wu G, Geng DY, Yin B. Differentiating primary central nervous system lymphomas from glioblastomas and inflammatory demyelinating pseudotumor using relative minimum apparent diffusion coefficients. *J Comput Assist Tomogr* 2017; 41:904–909
28. Lu SS, Kim SJ, Kim N, Kim HS, Choi CG, Lim YM. Histogram analysis of apparent diffusion coefficient maps for differentiating primary CNS lymphomas from tumefactive demyelinating lesions. *AJR* 2015; 204:827–834
29. Toh CH, Wei KC, Ng SH, Wan YL, Castillo M, Lin CP. Differentiation of tumefactive demyelinating lesions from high-grade gliomas with the use of diffusion tensor imaging. *AJNR* 2012; 33:846–851
30. Blasel S, Pfeilschifter W, Jansen V, Mueller K, Zanella F, Hattingen E. Metabolism and regional cerebral blood volume in autoimmune inflammatory demyelinating lesions mimicking malignant gliomas. *J Neurol* 2011; 258:113–122
31. Cha S, Pierce S, Knopp EA, et al. Dynamic contrast-enhanced T2*-weighted MR imaging of tumefactive demyelinating lesions. *AJNR* 2001; 22:1109–1116
32. Ikeguchi R, Shimizu Y, Abe K, et al. Proton magnetic resonance spectroscopy differentiates tumefactive demyelinating lesions from gliomas. *Mult Scler Relat Disord* 2018; 26:77–84
33. Lu SS, Kim SJ, Kim HS, et al. Utility of proton MR spectroscopy for differentiating typical and atypical primary central nervous system lymphomas from tumefactive demyelinating lesions. *AJNR* 2014; 35:270–277
34. Aboagye EO, Bhujwala ZM. Malignant transformation alters membrane choline phospholipid metabolism of human mammary epithelial cells. *Cancer Res* 1999; 59:80–84
35. Kiriya T, Kataoka H, Taoka T, et al. Characteristic neuroimaging in patients with tumefactive demyelinating lesions exceeding 30 mm. *J Neuroimaging* 2011; 21:e69–e77
36. Schiepers C, Van Hecke P, Vandenberghe R, et al. Positron emission tomography, magnetic resonance imaging and proton NMR spectroscopy of white matter in multiple sclerosis. *Mult Scler* 1997; 3:8–17
37. Bakshi R, Miletech RS, Kinkel PR, Emmet ML, Kinkel WR. High-resolution fluorodeoxyglucose positron emission tomography shows both global and regional cerebral hypometabolism in multiple sclerosis. *J Neuroimaging* 1998; 8:228–234
38. Takenaka S, Shinoda J, Asano Y, et al. Metabolic assessment of monofocal acute inflammatory demyelination using MR spectroscopy and ¹¹C-methionine-, ¹¹C-choline-, and ¹⁸F-fluorodeoxyglucose-PET. *Brain Tumor Pathol* 2011; 28:229–238
39. Yasuda S, Yano H, Kimura A, et al. Frontal tumefactive demyelinating lesion mimicking glioblastoma differentiated by methionine positron emission tomography. *World Neurosurg* 2018; 119:244–248
40. Ninomiya S, Hara M, Morita A, et al. Tumefactive demyelinating lesion differentiated from a brain tumor using a combination of magnetic resonance imaging and (11)C-methionine positron emission tomography. *Intern Med* 2015; 54:1411–1414
41. Nakajima R, Kimura K, Abe K, Sakai S. ¹¹C-methionine PET/CT findings in benign brain disease. *Jpn J Radiol* 2017; 35:279–288
42. Matsuzono K, Deguchi K, Hishikawa N, et al. Tumefactive demyelinating disease mimicking malignant tumor in positron emission tomography with ¹¹C-methionine. *Neurol Clin Neurosci* 2015; 3:81–83
43. Barbagallo M, Albatly AA, Schreiner S, et al. Value of ¹⁸F-FET PET in patients with suspected tumefactive demyelinating disease—preliminary experience from a retrospective analysis. *Clin Nucl Med* 2018; 43:e385–e391
44. Codjia P, Ayrignac X, Carra-Dalliere C, et al.; SFSEP and OFSEP. Multiple sclerosis with atypical MRI presentation: results of a nationwide multicenter study in 57 consecutive cases. *Mult Scler Relat Disord* 2019; 28:109–116
45. Jeong IH, Kim SH, Hyun JW, Joung A, Cho HJ, Kim HJ. Tumefactive demyelinating lesions as a first clinical event: clinical, imaging, and follow-up observations. *J Neurol Sci* 2015; 358:118–124

46. Qi W, Jia GE, Wang X, Zhang M, Ma Z. Cerebral tumefactive demyelinating lesions. *Oncol Lett* 2015; 10:1763–1768
47. Sinnecker T, Dörr J, Pfueller CF, et al. Distinct lesion morphology at 7-T MRI differentiates neuromyelitis optica from multiple sclerosis. *Neurology* 2012; 79:708–714
48. Cortese R, Magnollay L, Tur C, et al. Value of the central vein sign at 3T to differentiate MS from seropositive NMOSD. *Neurology* 2018; 90:e1183–e1190
49. Sati P, Oh J, Constable RT, et al.; NAIMS Cooperative. The central vein sign and its clinical evaluation for the diagnosis of multiple sclerosis: a consensus statement from the North American imaging in Multiple Sclerosis Cooperative. *Nat Rev Neurol* 2016; 12:714–722
50. Kilsdonk ID, Lopez-Soriano A, Kuijter JPA, et al. Morphological features of MS lesions on FLAIR* at 7 T and their relation to patient characteristics. *J Neurol* 2014; 261:1356–1364
51. Tan IL, van Schijndel RA, Pouwels PJW, et al. MR venography of multiple sclerosis. *AJNR* 2000; 21:1039–1042
52. Tallantyre EC, Brookes MJ, Dixon JE, Morgan PS, Evangelou N, Morris PG. Demonstrating the perivascular distribution of MS lesions in vivo with 7-Tesla MRI. *Neurology* 2008; 70:2076–2078
53. Absinta M, Nair G, Monaco MCG, et al. The “central vein sign” in inflammatory demyelination: The role of fibrillar collagen type I. *Ann Neurol* 2019; 85:934–942
54. Moritani T, Ekholm S, Westesson PA, eds. Demyelinating and degenerative disease. In: Moritani T, Ekholm S, Westesson PA. *Diffusion-weighted MR imaging of the brain*, 2nd ed. Springer, 2009:141–166
55. Hardy TA, Miller DH. Baló's concentric sclerosis. *Lancet Neurol* 2014; 13:740–746
56. Frederick MC, Cameron MH. Tumefactive demyelinating lesions in multiple sclerosis and associated disorders. *Curr Neurol Neurosci Rep* 2016; 16:26
57. Kishimoto R, Yabe I, Niino M, et al. Baló's concentric sclerosislike lesion in the brainstem of a multiple sclerosis patient. *J Neurol* 2008; 255:760–761
58. Ferreira D, Castro S, Nadais G, Dias Costa JM, Fonseca JM. Demyelinating lesions with features of Baló's concentric sclerosis in a patient with active hepatitis C and human herpesvirus 6 infection. *Eur J Neurol* 2011; 18:e6–e7
59. Graber JJ, Kister I, Geyer H, Khaund M, Herbert J. Neuromyelitis optica and concentric rings of Baló in the brainstem. *Arch Neurol* 2009; 66:274–275
60. Markiewicz D, Adamczewska-Gonczewicz Z, Dymecki J, Gonczewicz A. A case of primary form of progressive multifocal leukoencephalopathy with concentric demyelination of Baló type. *Neuropatol Pol* 1977; 15:491–500
61. Hardy TA, Corboy JR, Weinshenker BG. Baló concentric sclerosis evolving from apparent tumefactive demyelination. *Neurology* 2017; 88:2150–2152
62. Zabad RK, Stewart R, Healey KM. Pattern recognition of the multiple sclerosis syndrome. *Brain Sci* 2017; 7:E138
63. Jarius S, Würthwein C, Behrens JR, et al. Baló's concentric sclerosis is immunologically distinct from multiple sclerosis: results from retrospective analysis of almost 150 lumbar punctures. *J Neuroinflammation* 2018; 15:22
64. Poser CM, Goutières F, Carpentier MA, Aicardi J. Schilder's myelinoclastic diffuse sclerosis. *Pediatrics* 1986; 77:107–112
65. Miyamoto N, Kagohashi M, Nishioka K, et al. An autopsy case of Schilder's variant of multiple sclerosis (Schilder's disease). *Eur Neurol* 2006; 55:103–107
66. Jarius S, Haas J, Paul F, Wildemann B. Myelinoclastic diffuse sclerosis (Schilder's disease) is immunologically distinct from multiple sclerosis: results from retrospective analysis of 92 lumbar punctures. *J Neuroinflammation* 2019; 16:51
67. Hardy TA, Reddel SW, Barnett MH, Palace J, Lucchinetti CF, Weinshenker BG. Atypical inflammatory demyelinating syndromes of the CNS. *Lancet Neurol* 2016; 15:967–981
68. Weinshenker BG, Wingerchuk DM. Neuromyelitis spectrum disorders. *Mayo Clin Proc* 2017; 92:663–679
69. Jarius S, Paul F, Aktas O, et al. MOG encephalomyelitis: international recommendations on diagnosis and antibody testing. *J Neuroinflammation* 2018; 15:134
70. Katsuse K, Kurihara M, Sugiyama Y, et al. Aphasical status epilepticus preceding tumefactive left hemisphere lesion in anti-MOG antibody associated disease. *Mult Scler Relat Disord* 2019; 27:91–94
71. Tomizawa Y, Nakamura R, Hoshino Y, et al. Tumefactive demyelinating brain lesions with multiple closed-ring enhancement in the course of neuromyelitis optica. *J Neurol Sci* 2016; 361:49–51
72. Min JH, Kim BJ, Lee KH. Development of extensive brain lesions following fingolimod (FTY720) treatment in a patient with neuromyelitis optica spectrum disorder. *Mult Scler* 2012; 18:113–115
73. Saiki S, Ueno Y, Moritani T, et al. Extensive hemispheric lesions with radiological evidence of blood-brain barrier integrity in a patient with neuromyelitis optica. *J Neurol Sci* 2009; 284:217–219
74. Ikeda K, Ito H, Hidaka T, et al. Repeated non-enhancing tumefactive lesions in a patient with a neuromyelitis optica spectrum disorder. *Intern Med* 2011; 50:1061–1064
75. Roy U, Saini DS, Pan K, Pandit A, Ganguly G, Panwar A. Neuromyelitis optica spectrum disorder with tumefactive demyelination mimicking multiple sclerosis: a rare case. *Front Neurol* 2016; 7:73
76. Matsushita T, Isobe N, Matsuoka T, et al. Extensive vasogenic edema of anti-aquaporin-4 antibody-related brain lesions. *Mult Scler* 2009; 15:1113–1117
77. Akaishi T, Nakashima I, Sato DK, Takahashi T, Fujihara K. Neuromyelitis optica spectrum disorders. *Neuroimaging Clin N Am* 2017; 27:251–265
78. Ito S, Mori M, Makino T, Hayakawa S, Kuwabara S. “Cloud-like enhancement” is a magnetic resonance imaging abnormality specific to neuromyelitis optica. *Ann Neurol* 2009; 66:425–428
79. Tenenbaum S, Chitnis T, Ness J, Hahn JS; International Pediatric MS Study Group. Acute disseminated encephalomyelitis. *Neurology* 2007; 68(suppl 2):S23–S36
80. Torisu H, Kira R, Ishizaki Y, et al. Clinical study of childhood acute disseminated encephalomyelitis, multiple sclerosis, and acute transverse myelitis in Fukuoka Prefecture, Japan. *Brain Dev* 2010; 32:454–462
81. VanLandingham M, Hanigan W, Vedanarayanan V, Fratkin J. An uncommon illness with a rare presentation: neurosurgical management of ADEM with tumefactive demyelination in children. *Childs Nerv Syst* 2010; 26:655–661
82. Banwell B, Bar-Or A, Arnold DL, et al. Clinical, environmental, and genetic determinants of multiple sclerosis in children with acute demyelination: a prospective national cohort study. *Lancet Neurol* 2011; 10:436–445
83. Titulaer MJ, Höftberger R, Iizuka T, et al. Overlapping demyelinating syndromes and anti-N-methyl-D-aspartate receptor encephalitis. *Ann Neurol* 2014; 75:411–428
84. Luo JJ, Lv H, Sun W, et al. Anti-N-methyl-d-aspartate receptor encephalitis in a patient with neuromyelitis optica spectrum disorders. *Mult Scler Relat Disord* 2016; 8:74–77
85. Zhang W, Cui L, Wang W, Jiao Y, Zhang Y, Jiao J. Early identification of anti-NMDA receptor encephalitis presenting cerebral lesions in unconventional locations on magnetic resonance imaging. *J Neuroimmunol* 2018; 320:101–106
86. Faissner S, Hoepner R, Lukas C, Chan A, Gold R, Ellrichmann G. Tumefactive multiple sclerosis lesions in two patients after cessation of fingolimod treatment. *Ther Adv Neurol Disord* 2015; 8:233–238
87. Hellmann MA, Lev N, Lotan I, et al. Tumefactive demyelination and a malignant course in an MS patient during and following fingolimod therapy. *J Neurol Sci* 2014; 344:193–197

88. Beume LA, Dersch R, Fuhrer H, Stich O, Rauer S, Niesen WD. Massive exacerbation of multiple sclerosis after withdrawal and early restart of treatment with natalizumab. *J Clin Neurosci* 2015; 22:400–401
89. Yamamoto J, Shimajiri S, Nakano Y, Nishizawa S. Primary central nervous system lymphoma with preceding spontaneous pseudotumoral demyelination in an immunocompetent adult patient: a case report and literature review. *Oncol Lett* 2014; 7:1835–1838
90. Kvarta MD, Sharma D, Castellani RJ, et al. Demyelination as a harbinger of lymphoma: a case report and review of primary central nervous system lymphoma preceded by multifocal sentinel demyelination. *BMC Neurol* 2016; 16:72
91. Kalus S, Di Muzio B, Gaillard F. Demyelination preceding a diagnosis of central nervous system lymphoma. *J Clin Neurosci* 2016; 24:146–148
92. Ohe Y, Hayashi T, Mishima K, et al. Central nervous system lymphoma initially diagnosed as tumefactive multiple sclerosis after brain biopsy. *Intern Med* 2013; 52:483–488
93. Dasgupta N, Gelber AC, Racke F, Fine DM. Central nervous system lymphoma associated with mycophenolate mofetil in lupus nephritis. *Lupus* 2005; 14:910–913
94. Santucci GM, Leach JL, Ying J, Leach SD, Tomsick TA. Brain parenchymal signal abnormalities associated with developmental venous anomalies: detailed MR imaging assessment. *AJNR* 2008; 29:1317–1323
95. San Millán Ruíz D, Delavelle J, Yilmaz H, et al. Parenchymal abnormalities associated with developmental venous anomalies. *Neuroradiology* 2007; 49:987–995
96. Umino M, Maeda M, Matsushima N, Matsuura K, Yamada T, Sakuma H. High-signal-intensity abnormalities evaluated by 3D fluid-attenuated inversion recovery imaging within the drainage territory of developmental venous anomalies identified by susceptibility-weighted imaging at 3 T. *Jpn J Radiol* 2014; 32:397–404
97. Linscott LL, Leach JL, Zhang B, Jones BV. Brain parenchymal signal abnormalities associated with developmental venous anomalies in children and young adults. *AJNR* 2014; 35:1600–1607
98. Rogers DM, Shah LM, Wiggins RH 3rd. The central vein: FLAIR signal abnormalities associated with developmental venous anomalies in patients with multiple sclerosis. *AJNR* 2018; 39:2007–2013
99. Rogers DM, Peckham ME, Shah LM, Wiggins RH 3rd. Association of developmental venous anomalies with demyelinating lesions in patients with multiple sclerosis. *AJNR* 2018; 39:97–101
100. Weinschenker BG, O'Brien PC, Petterson TM, et al. A randomized trial of plasma exchange in acute central nervous system inflammatory demyelinating disease. *Ann Neurol* 1999; 46:878–886
101. Hardy TA, Chataway J. Tumefactive demyelination: an approach to diagnosis and management. *J Neurol Neurosurg Psychiatry* 2013; 84:1047–1053